PCCP

Accepted Manuscript

ROYAL SOCIETY OF CHEMISTRY

www.rsc.org/pccp

PCCP

ARTICLE

Effect of π–π interaction in Bergman Cyclisation†

Saibal Jana and Anakuthil Anoop*[a]

Received 00th January 20xx,
Accepted 00th January 20xx

DOI: 10.1039/x0xx00000x

www.rsc.org/

The role of π–π interactions in controlling the reactivity and selectivity of a chemical reaction is only recently being explored, even though their ubiquitous role in the structural aspects are well known. We have studied Bergman Cyclisation focusing on the role of π–π interactions in the activation barrier and the variation of π–π interactions along the reaction coordinate. We used enediyne substrates that contain phenyl groups connected to the reaction centres (C1 and C6 atoms), separated by 0, 1 and 2 linker groups. The main difference between the substrates is that the Ph groups enjoy different flexibility to accommodate the changes occuring during the progress of the reaction. The path length of the minimum energy path is increased–shortest in the least flexible substrate (**a**) and longer in the more flexible ones (**c**, **d** and **e**). We calculated the interaction between the Ph groups, the π–π interaction, using BP86-D3BJ, B3LYP-D3BJ, M06-2X, B2PLYP-D3BJ, SCS-MP2, and SAPT. The BP86-D3BJ was found to be sufficiently accurate with a Mean Absolute Deviation of 0.26 kcal/mol with respect to the SAPT2+3 values. The variation in the π–π interaction shows different behaviour in **a**-**e**, and the behaviour can be correlated with the flexibility of the Ph's to orient themselves to maintain the optimal relative orientation while conforming to the changes in the reaction coordinate. We analysed the relative orientation of the phenyl groups using certain geometric parameters that showed that when Ph's can attain a relative orientation close to that of the free dimer, the interaction is maximum. Energy decomposition analysis using SAPT, showed that the dispersive interaction is the major contributor (50-60%) to the attactive forces. The π–π interactions influenced the overall activation energy, either by destabilising the substrates or by stabilising the TS – resulting a variation of about 3.5 kcal/mol in activation energies in **a**-**e**. The effect of substituents of different electronic nature are assessed which shows that electron donating and electron withdrawing substituents, have increased the π–π interactions, however, the TS state is more stabilised and hence activation energies are increased.

1 Introduction

One of the recent and major interests in computational chemistry is to understand and characterise non–covalent interactions in various aspects of chemistry, biology and material science.[1] The significance of non–covalent interactions has been identified in the structure of macromolecules and in several natural phenomena. It has significant role in the geometrical organisation of tertiary protein structures, enzyme–substrate complexes, organic supramolecules and organic nanomaterials,[2,3,4,5,6,7,8] vertical base stacking in DNA[9,10,11,12] etc. Non-covalent interaections also contributes in several processes, such as intercalation of drugs into DNA, stabilisation of host-guest complexes[4,13] etc. Although non–covalent interactions are much weaker compared to electrostatic or covalent interactions, they are substantial, and their significance in several new domains are being revealed. For example, the weak interaction in halogen bonds[14] is a recent interest.

One such sub domain of weak non-covalent interactions is the attractive interaction present between aromatic units, termed as π–π (stacking) interaction. In molecular systems containing many aromatic groups in the vicinity (within ~5Å), the π–π interactions are crucial in the geometrical organisation,[15,16,17] and thus the structural aspects of π–π interactions has been a major interest among theoretical chemists.[18,19,20,21,22,23,24,25,26,27,28] But, their role in chemical reactions is relatively less explored, and reports in this direction are recently emerging.[29]

We can anticipate an effect of π–π interactions on the reactivity and selectivity of the reaction when two aromatic units are near the reaction centre – i.e. near the atoms that are involved in bond forming or bond breaking. This effect however, need not be always favourable, although π–π interaction is a stabilising interaction. For example, if the π–π interaction stabilises only the substrate geometry, and not the transition state, the activation energy will be higher in this system compared to the systems having no π–π interactions. On the other hand, if the interactions are significant only in the transition state, the activation energy will decrease. Again, if it is effective only in the product geometries, the reaction will be benefited if the reaction is under thermodynamic control.

[a] Department of Chemistry, Indian Institute of Technology Kharagpur, Kharagpur 721302, India, E-mail: anoop@chem.iitkgp.ernet.in, Tel: +91.3222283316

† Electronic Supplementary Information (ESI) available: See DOI: 10.1039/x0xx000x

Thus, we can imagine that the π–π interactions can favour the reactivity or selectivity by: a) pre-organisation of substrates, b) lowering activation barriers, or c) thermodynamic stabilisation of products.

The importance of pre-orienting the substrates was established by the computational studies from our group, in the case of Garratt-Braverman cyclisations.[30] This became more evident when the steric bulk or other repulsive interactions prevent the formation of π–π stacked substrates, the selectivity is changed towards the other competitive cyclisation pathways.[31] The other scenario, where the selectivity of the reaction is controlled by the π–π interactions in the transition state geometry is recently reviewed by Krenske and Houk.[29] Understanding the effect of π–π interactions in the whole spectrum – from substrate to products – will be beneficial in getting the overall picture.

The aim of our work is to investigate the variation of π–π interactions along the reaction coordinate of a chemical reaction. This was done by studying a model system containing aromatic units near the reaction centre. The interactions between the aromatic units are often modelled using the π–stacked benzene dimer. Three prototype orientations are studied extensively – parallel displaced and T-shaped orientations are minima, and the sandwich orientation is a saddle point connecting those minima.[32,33,34,35,36] These two minima are roughly isoenergetic with less than 0.1 kcal/mol of energy difference, and the interaction energy of the dimer is about –2.5 to –3.0 kcal/mol.[34,35,37] In our model study, we have focussed on the nearly parallel arrangement of the dimers; the T-shaped dimer is not considered here.

As a model reaction for this study, we considered thermal cyclisation of polyunsaturated hydrocarbons, which has the advantage of being relatively less affected by various complex effects of solvents, catalysts etc. Moreover, mechanistic studies on cyclisation reactions are always relevant as these reactions follow the atom–economic route to generate complex carbocycles and heterocycles. We have chosen Bergman Cyclisation (BC) as our model reaction, which has a vast literature on various aspects of the mechanism.[38,39,40]

The studies, reviewed by Kraka and Cremer,[38] Alabugin *et al.*,[39] and many others, show that the factors that control the BC reaction are, proximity, strain, and electronic effects. Any geometrical factors that can bring the C1-C6 distance (Scheme 1) below 3.2 Å (proposed by Nicolaou[41] from empirical studies) can enhance the rate of BC considerably. Rate enhancement can also be achieved by incorporating strain in the molecule, which either destabilise the substrate or stabilise the transition state (TS). Substituents with electron donating or withdrawing characters also affect the rate of the reaction.

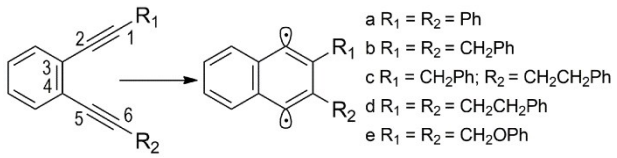

Scheme 1 Bergman Cyclisation; R_1 and R_2 represent different functional groups.

We studied the variation of interactions between the aromatic rings during the chemical reaction when the substrate is converted to the TS, and to the product which is a biradical intermediate in our case. For this, we optimised a minimum energy path (MEP) for the BC reaction of the model systems (**a**-**e** in Scheme 1). From the geometries along MEP, we have extracted the 'benzene dimer' units (see computational methods for details), which are used for the detailed study of π–π interactions. The interaction energy is computed using several methods: popular density functionals, wave function based methods, and symmetry adapted perturbation theory (SAPT). Using Energy Decomposition Analysis (EDA) in the SAPT, we have examined various contributions to the interaction energy. Non–Covalent Interaction (NCI) analysis was done for the substrate, transition state and corresponding intermediate geometry to visualise the π–π interactions. The contribution of π–π interactions to the activation energy is discussed. We further studied the electronic effects using models containing electron-donating and electron-withdrawing substituents. This study exhibit many novel features of Bergman cyclisation and the π-π interactions.

2 Computational Details

2.1 Electronic Structure Calculations

Energies and gradients for the optimisation of the potential energy surfaces were evaluated using BP86-D3BJ/def2-TZVPP level of theory. This method involve the pure GGA functional, BP86[42,43] and triple-ζ quality basis set, def2–TZVPP[44], and third generation of Grimme's empirical dispersion correction, with Becke–Johnson damping function[45]. This level of theory is popular as a fast, efficient and sufficiently accurate method[46] for optimisation of large molecules. Moreover, pure GGA functionals are shown to perform well for the biradical systems.[47] Interaction energies were evaluated using some of the frequently used methods for non-covalent interactions such as, the hybrid functionals (B3LYP-D3BJ[48,49] and M06-2X[50]), double-hybrid functional (B2PLYP-D3BJ[51]), and spin-component scaled Møller-Plesset perturbation theory (SCS-MP2[52]) methods. We have used unrestricted formalism to account the biradical character of the intermediates. Spin density analysis clearly show the biradical nature and the spin contamination in all the intermediate geometries are less than < 1%. Basis Set Superposition Error (BSSE) is not considered in our calculations, because it is reported[53] that while using DFT-D methods with triple-ζ quality basis sets, BSSE calculations can be avoided, while BSSE correction is essential in case of highly correlated methods.[54,55] All the electronic structure calculations are performed in Orca 3.0.0,[56] and in Turbomole 6.5[57]

2.2 Model Systems

Five model substrate compounds (**a**-**e**; Scheme 1) were selected for our study of the effect of π–π interactions in chemical reactions. These enediyne substrates, **a**-**e**, contain two terminal phenyl groups which are connected to the alkynyl

group, either directly (as in **a**), or through linking groups, -CH_2- (**b**), -CH_2CH_2-(**d**), or -CH_2O-(**e**). Two different linkers, one –CH_2- and one -CH_2CH_2- , are used in **c**. The phenyl groups are kept in a stacked or nearly stacked orientation in the initial substrate geometry.

The substrate **b** is modified with substituents – electron withdrawing -F and electron donating -NH_2 in *ortho* and *meta* positions – to study the electronic effect of substituents on the π–π interactions. To minimise the direct interaction among the substituents, *ortho* and *meta* positions on the opposite sides of Ph are substituted, while *para* position is kept unsubstituted. In **b1**, *ortho* and *meta* positions of both phenyl rings are substituted with electron withdrawing -F to make the rings less electron dense, while in **b2**, electron donating groups (-NH_2) are used that make the rings more electron dense. And in **b3**, one phenyl ring is substituted with -F, and the other ring is substituted with –NH_2.

2.3 Minimum Energy Path

The substrate geometries for each of the model systems (**a**-**e**) were subjected to a relaxed surface scan in which the distance between the reacting carbons is reduced in steps keeping the remaining coordinates free (unconstrained). The final geometries from the scan are fully optimised and were used as the product of the cyclisation step. Further optimisation of the reaction path is carried out using CI-NEB algorithm[58]. The nudged elastic band (NEB) is a method for finding transition states and MEP's between reactants and products. The algorithm optimises a number of intermediate images – we used 17 – along the reaction path. Each image is optimised to minima while maintaining equal spacing to neighbouring images. This constrained optimisation is done by adding spring forces along the band between images and by projecting out the component of the force due to the potential perpendicular to the band. The highest energy image is driven up to the saddle point. Transition state (TS) geometry provided by CI-NEB method is further optimised for TS, and characterised using normal mode vibrational analysis. Relaxed Surface scan, TS optimisation and Minimum Energy Path (MEP) calculations were done using DL-Find optimizer[59] implemented in Chemshell 3.5[60].

2.4 Estimating the π–π Interaction Energies

From each point in the MEP, we have calculated the π–π interaction energy ($IE_{\pi-\pi}$) of the *benzene-dimer*. To build the geometry of the *benzene-dimer*, we extracted the atomic coordinates of the two phenyl groups from the cartesian coordinates of the complete geometry. This created a dangling valency in one of the phenyl carbon atoms that was connected with the enediyne core. We added a hydrogen atom at a fixed distance to fill this valency. Then $IE_{\pi-\pi}$ was calculated as the difference in energy between the benzene dimer and the sum of the single point energies of benzene monomers calculated separately.

$$IE_{\pi-\pi} = E_{dimer} - (E_{monomer\ 1} + E_{monomer\ 2}) \quad (1)$$

We calculated $IE_{\pi-\pi}$ for 17 geometries obtained from the MEP of the cyclisation using the following methods: BP86-D3BJ, B3LYP-D3BJ, M06-2X, B2PLYP-D3BJ, and SCS-MP2.

2.5 Symmetry Adapted Perturbation Theory (SAPT)

Computation of $IE_{\pi-\pi}$ using equation (1) is known as supermolecular method. SAPT is a powerful tool that can calculate the interaction energy directly and also can get further insight about the interaction energy in terms of its various physically meaningful components: electrostatic, exchange, induction, and dispersion. SAPT directly computes the non-covalent interactions between two molecules, that is, the interaction energy is determined without computing the total energy of the monomers or dimer. In this approach, the Hamiltonian is partitioned into monomer Fock operators, Møller-Plesset fluctuation operators (representing intramolecular electron correlation), and the intermolecular interaction operators. High order terms of fluctuation potential and intermolecular interaction are required to get accurate interaction energy. Several truncations of the SAPT expansion are available. They are SAPT0, SAPT2, SAPT2+, SAPT2+(3) and SAPT2+3 etc. Among these we have considered the highest level of SAPT, i.e SAPT2+3 results for our discussion.

We have also carried out energy decomposition analysis (EDA) in the SAPT scheme, on the benzene dimers obtained from the PES, to get more insights on the variation of different contributions to the interaction energy during the cyclisation reaction. The density fitting SAPT calculations are carried out using the PSI4 program.[61] The EDA separates the overall interaction energy between two aromatic rings in terms of their contributions from electrostatic (E_{es}), exchange-repulsion (E_{ex}), induction (E_{ind}), and dispersion (E_{disp}) energy.

2.6 Non-Covalent Interaction (NCI) Index

While SAPT gives us a rigorous analysis of interaction energy, it will be helpful to also have qualitative visualisation of non-covalent interactions. Non–covalent interaction (NCI) index, recently introduced by Yang and co–worker[62], is such a tool which is capable of mapping the non-covalent interactions zone in real space qualitatively. The method is based on the two scalar fields to map the bonding properties, the electron density (ρ) and reduced density gradient (RDG, s), defined as:

$$s = \frac{1}{2(3\pi^2)^{1/3}} \frac{|\nabla\rho|}{\rho^{4/3}} \quad (2)$$

The combination of s and ρ allows a rough partitioning of real space into bonding regions: high–s low–ρ corresponds to non–interacting density tails, low–s high–ρ to covalent bonds, and low–s low–ρ to non-covalent interactions.

From NCI plot it is easy to distinguish the H–bonding, van der Waals and steric interactions. At low–ρ and at low–s the non covalent interaction area is defined. The low RDG value at the negative low ρ is attractive zone and low RDG with positive low ρ are repulsive zone. Particularly, the trough at $-0.02 < \rho < 0.02$ are for the van der Wall interaction, $-0.06 < \rho < -0.04$ are for H–bond, and $0.04 < \rho < 0.08$ are for steric clashes. We have

carried out NCI analysis on the substrate, TS and biradical intermediate on one of our model systems (**b**) using NCIPLOT software.

3 Results and Discussion

3.1 Minimum Energy Path

Potential energy surface (PES) along the MEP for the cyclisation step starting from stable optimised substrate geometry to the corresponding intermediate for **a**-**e** is plotted in Figure 1. Energy is plotted against path length, which is an integrated Euclidean distance along the path. Substrate **a** with shortest path length undergoes minimal overall change in geometry on going from substrate to product. The path is longer for **b** than for **a**, as one CH_2 group between Ph groups and reaction centres (C1 and C6) gives more flexibility compared to **a**. The increase in flexibility when the Ph groups are further away from reaction centres in **c**-**e** is also visible in their longer path lengths.

Along the reaction coordinate, the energy changes marginally up to half of the path, up to ~3.2 Å of C1-C6 distance, followed by a sudden increase towards the TS. At a distance of 3.2 Å, the 4-electron repulsive interaction between the π-orbitals of alkynes is dominant over the two-electron bond-forming interaction, shown by Alabugin and Manoharan[63] using computational studies. The highest point in the PES is located toward the end (14^{th}-16^{th} image), indicating a late transition state, as expected for an endothermic step. The variations among the substrates can mostly be attributed to the differences in the functional groups, because all of these substrates have the same enediyne core. In **b**, there is almost no change till 10^{th} image, i.e., up to 3.5 Å of C1-C6 distance. In this region, the changes in the enediyne core are balanced by the changes in benzyl groups such that the total energy is maintained. On close look at the relative orientation of the phenyl groups, we noticed a movement towards more stable parallel-displaced benzene-dimer geometry. In the next section, we will analyse the interaction energy between the phenyl groups.

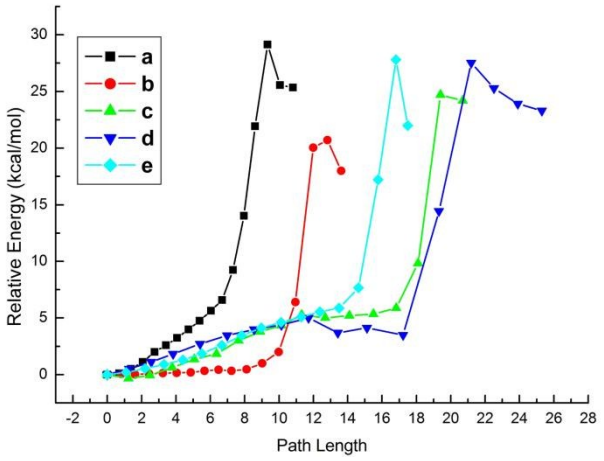

Figure 1 Potential energy surface of the Bergman cyclisation of a-e using the BP86-D3BJ/def2-TZVPP.

3.2 Interaction Energy

We calculated the interaction energy (IE) between two phenyl rings to determine the contribution of π–π interactions to the total energies. The IE between the benzene dimer that was extracted from the geometry of the complete molecule is calculated using supermolecular method and perturbative method, as described in the Computational methods section.

3.2.1 Supermolecular Interaction Energy

In this method, the IE is calculated as the energy difference between the benzene–dimer and the sum of two benzene monomers. The variation in interaction energy, calculated with BP86-D3BJ, B3LYP-D3BJ, M06-2X, B2PLYP-D3BJ, and SCS-MP2 and with def2-TZVPP basis set along the MEP are plotted in Figure 2. The complete data including the geometrical parameters of the benzene dimers are given in Supporting Information, Table 41-45. In all cases the computed IE is the largest with BP86-D3BJ, followed by SCS-MP2, B2PLYP-D3BJ, B3LYP-D3BJ, and M06-2X. Energies from all the methods follow the same trend.

3.2.2 Interaction energy from SAPT

We used symmetry adapted perturbation theory (SAPT) to calculate the interaction energies from perturbative theory. Figure 3 shows a comparison of the interaction energy obtained from SAPT2+3 and from supermolecular methods. BP86-D3BJ, our choice for the optimisation, performed well with a Mean Absolute Deviation of 0.26 kcal/mol with respect to the SAPT2+3 values. This shows the reliability of BP86-D3BJ for such calculations.

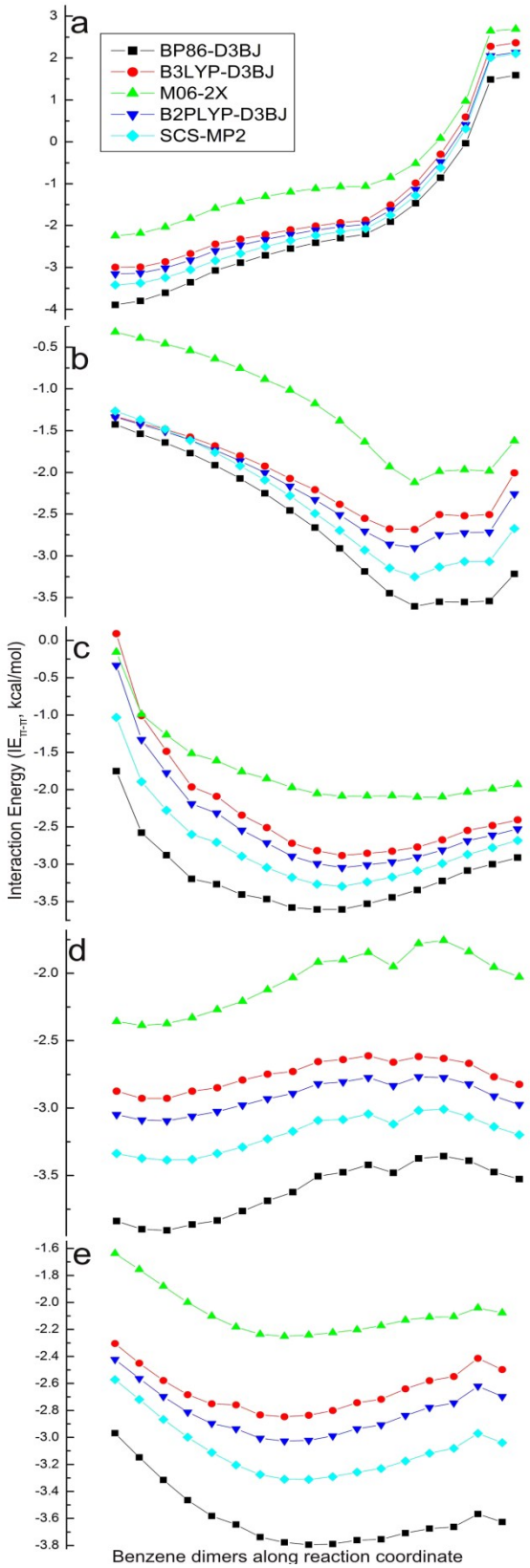

Figure 2 Interaction energy (IE) of the benzene-dimers along the reaction coordinates of Bergman cyclisation for **a**-**e** (calculated at BP86-D3BJ, B3LYP-D3BJ, M06-2X, B2PLYP-D3BJ, and SCS-MP2) using def2-TZVPP basis set.

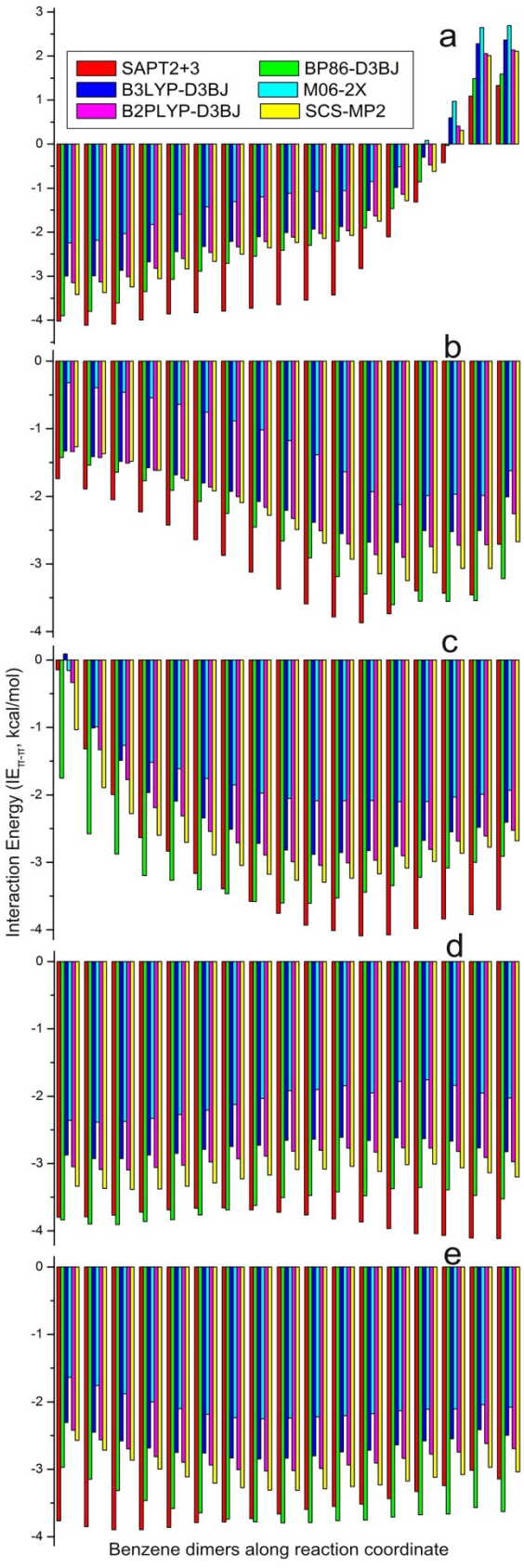

Figure 3 Interaction energy (IE) from DFT (BP86-D3BJ, B3LYP-D3BJ, M06-2X, B2PLYP-D3BJ), SCS-MP2 and SAPT2+3 calculations of the benzene dimers along the reaction coordinates of Bergman cyclisation.

3.2.3 General Features

The variation of IE along the PES for **a**-**e** calculated at BP86-D3BJ/def2-TZVPP level of theory is shown in Figure 4.. In the substrate **a** (R_1 = R_2 = Ph), when the phenyl groups are directly connected to the reaction centres (C1 and C6), the IE is maximum at the starting geometry and gradually decreases toward the corresponding biradical intermediate. In the last two images, the interaction is unfavourable. Moving the Ph groups further away from reaction centre, as in **b** (R_1 = R_2 = CH_2Ph), the interaction energy is gradually increased along the path and is maximum near the transition state. When Ph groups are even further away from reaction centre, in (**d**) (R_1 = CH_2CH_2Ph, R_2 = CH_2CH_2Ph), there is only a small variation of interaction energy compared to the previous cases. The interaction remains almost constant, with a slight decrease in the middle of the MEP. In **e**, (R_1 = CH_2OPh, R_2 = CH_2OPh), the spacer length is similar to **d**, but one of the CH_2 groups is replaced by O. The interaction energy remains almost constant in **e**, but with a small increase in the middle. In **c**, one linker is longer (R_1 = CH_2CH_2Ph) than the other (R_2 = CH_2Ph); the interaction increases as the reaction proceeds from the substrate geometry, reaches a maximum in the middle and then decreases slightly. Comparing all the systems (**a**-**e**), it is evident that the interaction between the phenyl groups varies differently in different systems (Figure 4).

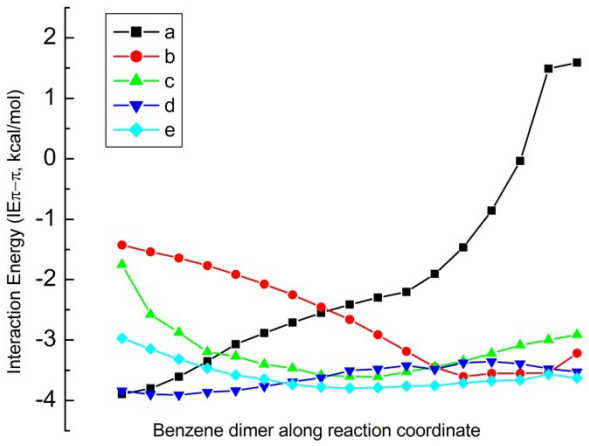

Figure 4 Interaction energy (IE) of the benzene dimers along the reaction coordinates of Bergman cyclisation for all five model systems plotted together. The IE's are calculated at BP86-D3BJ/def2-TZVPP level of theory.

3.3 Energy Decomposition Analysis

Interaction energy can be further decomposed into various terms: electrostatic, induction and dispersion. Figure 5 shows the relative contribution of these terms to the attractive interaction. In the substrate **a**, the contribution to attractive interaction from electrostatic interaction (E_{es}) is around 30-40%, and from inductive effects (E_{ind}) is 7-10%. Dispersive interaction (E_{disp}) is the highest (50-60%) contributor to the attractive interaction. The overall interaction energy in the last two points in the PES of **a** is repulsive, due to the large exchange interaction.

Similarly, in all the cases, the contribution from dispersive interaction to the attractive forces is major. In **b**, the contributions from different components are, E_{es} = 24-33%, E_{ind} = 6-8%, and E_{disp} = 60-70%. The contribution from the E_{disp} is more in **b** by around 10% than in **a**. In **c**, the contribution from E_{disp} is higher in the intermediate images. In case of **d** and **e**, the E_{disp} contribution decreases on going from substrate to product geometry. **See Supporting Information** for the complete data.

3.4 Geometrical changes

The change in interaction energy is associated with the changes in relative orientation of phenyl groups along the reaction coordinate in which the C-C bond formation takes place. The orientation of the phenyl group is more perturbed when Ph is nearer to the reaction centre. When phenyl groups are directly connected to the reaction centres as in **a**, the product has two Ph's in the vicinal position, and hence the interaction becomes repulsive in the product. In the remaining systems (**b**-**e**), the phenyl groups are relatively free to move. Therefore, they orient themselves in order to have maximum favourable interactions. We used three geometrical parameters to analyse these changes: a) distance (d_1), between the centroids of the phenyl groups b) parallel displacement (d_2) between the phenyl groups (which measure the deviation from the sandwich orientation), and c) angle between the two planes of phenyl rings (θ) (Figure 6).

These parameters (d_1, d_2 and θ) have their optimal values in the free-benzene-dimer. Figure 7 shows that when each of these parameters is close to the corresponding values of the free-benzene-dimer, the interaction is maximum and as they move away the interaction is reduced. In **d** and **e**, Ph groups are separated from the reaction centre by two atomic centres, and hence the geometrical parameters (d_1, d_2, and θ) and the IE are similar to the reference (free-dimer) values. Larger changes from the reference values of the parameters are seen in **a** and **b**, and the IE's are also varied in larger extents.

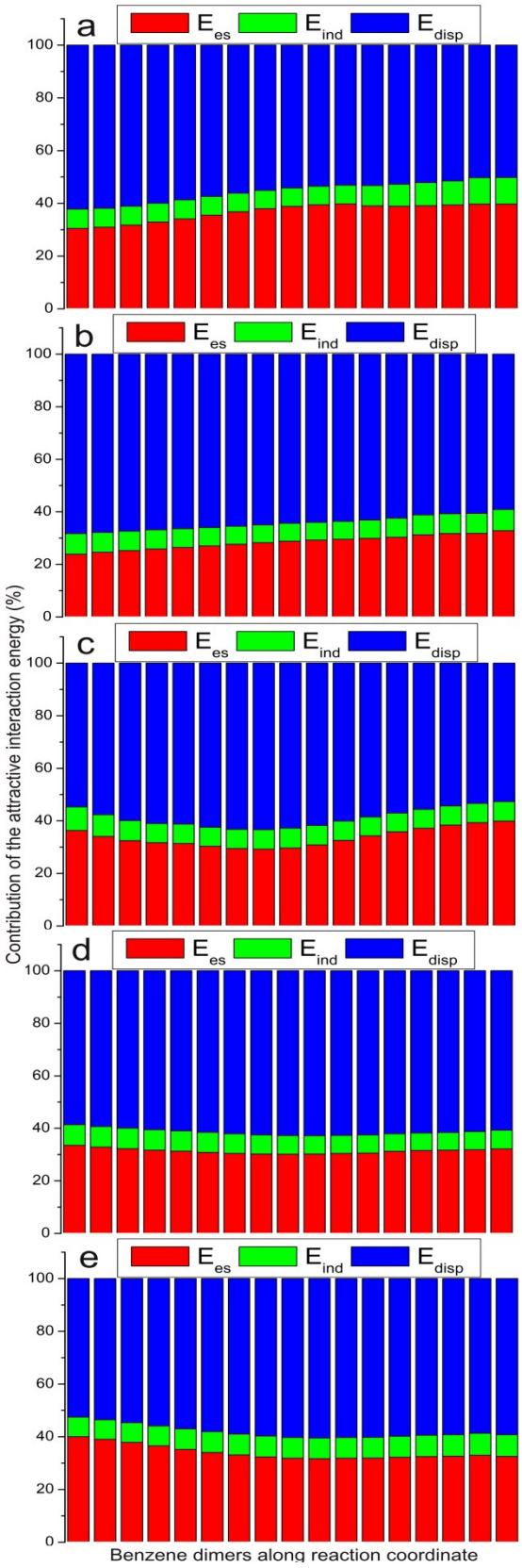

Figure 5 Contribution of different attractive interactions (%) at SAPT2+3 level towards the stability of π-π interaction energy (IE) of the benzene dimers along the reaction coordinates of Bergman cyclisation.

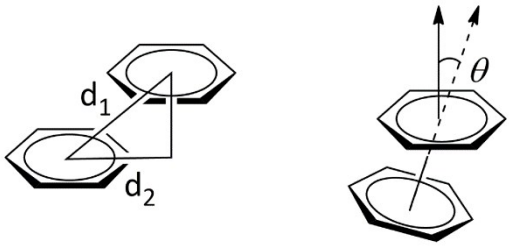

Figure 6 d_1 is the direct distance between centroids of each planes, d_2 represent the deviation from sandwich geometry, and θ is the angle between two planes.

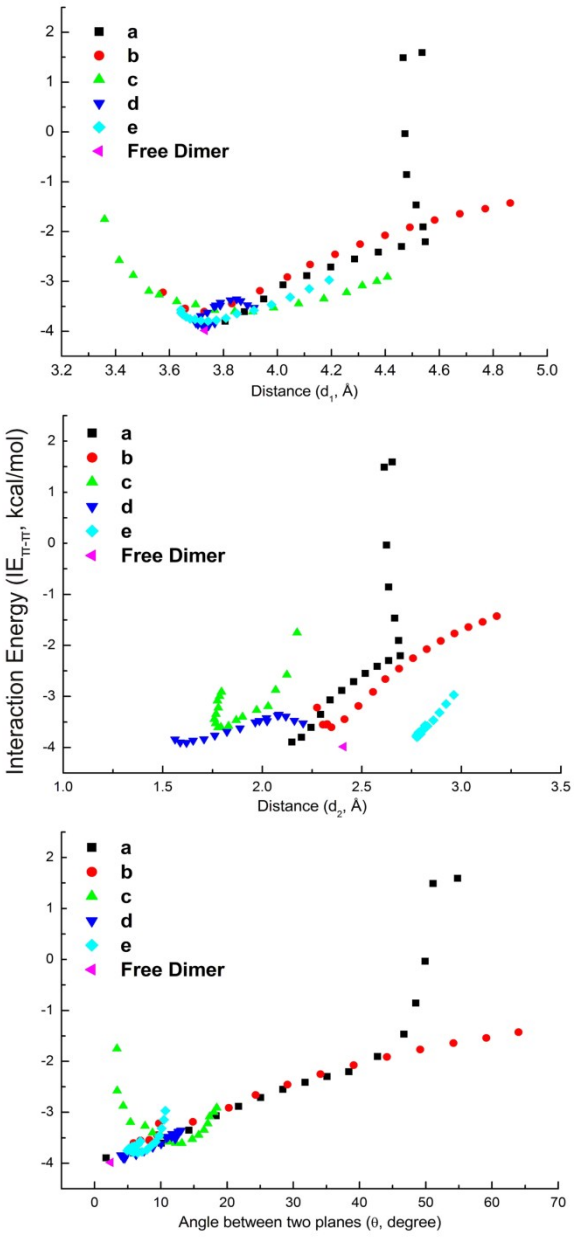

Figure 7 Interaction energy (IE, BP86-D3BJ/def2-TZVPP) plotted with respect to the distances (d_1 and d_2) and angle (Figure 6) along the reaction coordinates of Bergman cyclisation. Optimised geometry of free benzene dimer is shown in pink colour as a reference point for the most stable arrangement.

3.5 Reaction Energies and Activation Energies

After analysing the π-π interaction energy and their variation along the MEP, we analysed the contribution of π-π interactions to the overall reaction energy ($\Delta_r E$) and activation energy ($\Delta^{\ddagger}E$) (Table 1). The cyclisation step is endothermic (17.43-22.45 kcal/mol), as this step produces a reactive intermediate, a biradical. The activation energy values are between 27.58 and 31.06 kcal/mol.

The variations in energies can be illustrated in terms of the differences in the substrate structures, i.e. the difference in the number of groups between the reaction centre (C1 and C6) and phenyl groups. When Ph is directly attached to C1 and C6 in **a**, the $\Delta^{\ddagger}E$ is 31.06 kcal/mol, which is the highest among all activation energies. When one $-CH_2-$ group separates the reaction centres and Ph (**b**), the $\Delta^{\ddagger}E$ is 27.58 kcal/mol, which is the lowest among all. The spacer length is two in **d** and **e**. In both cases $\Delta^{\ddagger}E$ is in between that of **a** and **b**. When both linkers are ethylenes ($-CH_2-CH_2-$) in **d**, the $\Delta^{\ddagger}E$ is higher (30.96 kcal/mol) than the $\Delta^{\ddagger}E$ when both linkers are $-CH_2-O-$ in **e** ($\Delta^{\ddagger}E$ = 29.82 kcal/mol) – electronic effect of oxygen may contribute to this difference of 1.14 kcal/mol. When one linker is methylene and the other is ethylene in **c**, the $\Delta^{\ddagger}E$ is 30.17 kcal/mol, which is higher than **e** and lower than **d**.

Table 1 The activation energy ($\Delta^{\ddagger}E$), reaction energy ($\Delta_r E$) of the cyclisation for **a**-**e**. Change in interaction energy from substrate to TS is calculated as $\Delta IE_{\pi-\pi} = IE_{TS} - IE_{substrate}$. Distance between C1 and C6 in the substrate and transition state geometry. All energies are from BP86-D3BJ/def2-TZVPP calculation and are in kcal/mol.

Entry	System	Energy (kcal/mol)			C1-C6 distance (Å)	
		$\Delta^{\ddagger}E$	$\Delta IE_{\pi-\pi}$	$\Delta_r E$	Substrate	TS
a	R_1 = Ph; R_2 = Ph	31.06	3.46	22.45	3.890	1.836
b	R_1 = CH_2Ph; R_2 = CH_2Ph	27.58	-0.66	17.43	3.851	1.908
c	R_1 = CH_2CH_2Ph; R_2 = CH_2Ph	30.17	0.22	20.48	3.970	1.907
d	R_1 = CH_2CH_2Ph; R_2 = CH_2CH_2Ph	30.96	-0.48	22.12	3.708	1.889
e	R_1 = CH_2OPh; R_2 = CH_2OPh	29.82	-0.84	19.05	3.973	1.917

The attractive interactions between the phenyl groups pull the bond-forming carbon atoms (C1 and C6) nearer. All the C1-C6 distances in the substrates **a**-**e** are in the range of 3.71-3.97 Å, shorter than the C1-C6 distance in unsubstituted enediyne (R_1 = R_2 = H), 4.14 Å, and in methyl substituted substrate (R_1 = R_2 = Me), 4.11 Å. Although the π-π interactions help in bringing the C1 and C6 nearer, the C1-C6 distances do not approach the Nicolaou threshold[41] (see introduction) of 3.2 Å and hence we do not see a dramatic decrease in the activation energy. We do not expect such a proximity effect, because the distance between the two planes in the freely optimised, parallel-displaced benzene dimer is only 3.73 Å. In the TS, however, the C1-C6 distances are below 1.92 Å, and when the Ph groups are close to the C1 and C6, as in **a**, the interaction becomes repulsive (+2.57 kcal/mol). The result is that the $\Delta^{\ddagger}E$ is highest in **a**.

The contribution of π–π interaction energy ($IE_{\pi-\pi}$) on the activation energy ($\Delta^{\ddagger}E$) can be measured as the difference in $IE_{\pi-\pi}$ between the substrate and TS ($\Delta IE_{\pi-\pi} = IE_{TS} - IE_{substrate}$). In **a**, the substrate geometry has a $IE_{\pi-\pi}$ of -2.57 kcal/mol, and in TS it is 0.89 kcal/mol. The $\Delta IE_{\pi-\pi}$ is 3.46 kcal/mol which is the highest among **a**-**e**. The highest $\Delta IE_{\pi-\pi}$ match with the highest activation energy ($\Delta^{\ddagger}E$ = 31.06 kcal/mol) for **a**. The second highest activation energy is for **d**, which also has a positive $\Delta IE_{\pi-\pi}$ of 0.48 kcal/mol – i.e., the TS has less stabilisation from π–π interactions compared to the stabilisation in substrate. In the remaining systems, **b, c** and **e**, the TS are more stabilised than the substrate by π–π interactions. Consequently, the activation energy is lower than that of **a** and **c**. Thus the variations in π-π interaction can cause a difference of about 3.5 kcal/mol in activation energy.

3.6 NCI-plot analysis

Non-Covalent Interaction (NCI) analysis is helpful for visualising the variations in the interactions on going from substrate to the corresponding intermediate through the TS. Figure 8 presents the NCI plots of the substrate, TS and intermediate of **b** (R_1 = R_2 = CH_2Ph), showing the regions of the attractive intramolecular interactions. In the Figure 8, the trough at $-0.02 < \rho < 0.00$ are for the weak non-covalent van der Waals interactions. From substrate to the TS, the Reduced Density Gradient (RDG) in the region $0.0 > \rho > -0.02$ is increased, which shows the increase in attractive interaction between two aromatic rings. Again from TS to corresponding intermediate the change is negligible, i.e., the interactions in TS and the intermediate are similar.

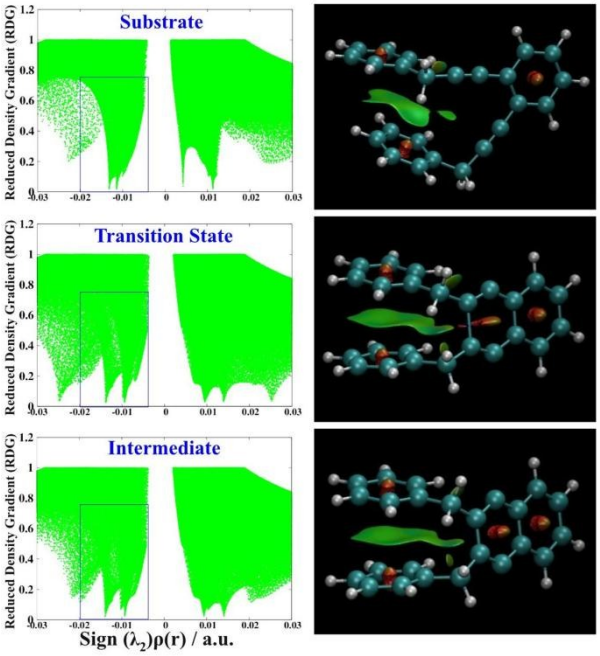

Figure 8 NCI analysis for the starting geometry of the model molecule. The flat green surface indicates π–π interaction between two aromatic rings. Left: Reduced density gradient versus the electron density multiplied by the sign of the second Hessian eigenvalue (λ_2). Right: gradient isosurface with s = 0.5 a.u.

3.7 Electronic effect

To study the electronic effect of substituents on the activation energy and on the π–π interactions, we used three model systems that are derived from **b**: **b1** (containing electron withdrawing substituents, F), **b2** (containing electron donating substituents, NH_2), and **b3** (F in one Ph, and NH_2 in the other). These substitutions affect the activation barrier ($\Delta^{\ddagger}E$) for the BC. Compared to the $\Delta^{\ddagger}E$ for **b**, the **b1** has 2.96 kcal/mol lower barrier, whereas the **b2** and **b3** have 5.28 and 5,19 kcal/mol higher barrier respectively-.

Table 2 Analysis of electronic effects using substrates, **b1**, **b2** and **b3**. All energies are from BP86-D3BJ/def2-TZVPP calculations and are in kcal/mol. Change in interaction energy from substrate to TS is calculated as $\Delta IE_{\pi-\pi} = IE_{TS} - IE_{substrate}$. Relative activation energy $\Delta\Delta^{\ddagger}E_{(b\ -\ bn)}$ is calculated as $\Delta^{\ddagger}E$(b) - $\Delta^{\ddagger}E$(bn); n = 1, 2 and 3. Relative π–π interaction energy with respect to **b**, $\Delta IE_{\pi-\pi}$ (b-bn) = $IE_{\pi-\pi}$(b) - $IE_{\pi-\pi}$(bn). ΔIE_{ISO} (b-bn) gives the relative energy from isodesmic equation, see supporting information for the equation.

Entry	$\Delta^{\ddagger}E$	$\Delta IE_{\pi-\pi}$ [a]	$\Delta\Delta^{\ddagger}E_{(b\ -\ bn)}$ [b]	$\Delta IE_{\pi-\pi}$ (b - bn) [c]		ΔIE_{ISO} (b - bn) [d]	
				sub	TS	sub	TS
b1	24.62	-3.08	2.96	-0.35	2.08	3.88	0.92
b2	32.86	1.54	-5.28	3.74	1.54	-5.38	-0.10
b3	32.76	1.24	-5.19	4.23	2.34	-1.94	3.24

[a] Positive values indicate that substrate is more stabilised than TS by π-π interaction. [b] Positive values means **b** has higher activation energy compared to bn. [c] Positive values imply that **bn** is more stable than **b**. [d] Positive values represent more stability for **bn** compared to **b**.

The decrease in $\Delta^{\ddagger}E$ of tetrafluoro substituted **b1**, is mainly coming from the destabilisation of substrate. Using isodesmic equations (see supporting information), the destabilisation of substrate is calculated to be 3.88 kcal/mol. The TS is also destabilised by 0.98 kcal/mol, resulting in the overall lowering of activation barrier by 2.96 kcal/mol. Out of this, 2.43 kcal/mol come from the differences in the stabilisation by π–π interactions in the **b1**, and rest come from the direct electronic effect of the substituents. Substitution increased the π–π interaction mainly in the TS.

Tetraamino substitution in **b2**, increased the activation barrier by 5.28 kcal/mol, which can be divided into the contribution from stabilisation of the substrate (5.38 kcal/mol) and the destabilisation of the TS (0.10 kcal/mol). Here both the substrate and TS are more stabilised by π–π interaction compared to **b**, but substrate is relatively more stabilised than TS by 2.20 kcal/mol.

Mixed substitution (F in one Ph and NH_2 in the other) also increased the activation barrier by 5.18 kcal/mol in **b3**. Although the barriers are similar in **b2** and **b3**, the contributions are different. Here in **b3**, the TS is destabilised by 3.24 kcal/mol, and the substrate is stabilised by 1.94 kcal/mol. Although the π–π interaction stabilised the TS compared to **b** (2.34 kcal/mol), overall TS is destabilised by 3.24 kcal/mol.

All the substituents have increased the π–π interaction in substrate and TS – except for the substrate of **b1** where the geometry did not favour the stacking orientation. The increase in π–π interaction irresptive to the electronic nature of the substituents is in agreement with the conclusion from Wheeler and Houk[64] that substituent effects in the benzene dimer are due to direct interaction of the substituent with the aromatic ring, and that the π-system of the substituted benzene is not involved.

4 Conclusions

We have studied the variation of π–π interactions along the reaction coordinate of Bergman Cyclisation. We used model substrates (**a**-**e**), in which, two phenyl groups are placed at increasing separations from the reaction centre making them increasingly flexible. The path length of the MEP increased with the flexibility. The energies along the MEP gradually increased until the C1-C6 distance of ~3.2 Å, followed by a steep increase towards the TS. The interaction between the aromatic rings were calculated using density functional theory and wave function theory based methods, and also by symmetry adapted perturbation theory (SAPT). With reference to SAPT2+3 interaction energies, BP86-D3BJ performed reasonably well. The π–π interaction varied differently in different substrates, and the behaviour can be correlated with their flexibility to orient themselves to maintain the optimal relative orientation while accommodating the changes in the reaction coordinate. The analysis of the geometric parameters representing the relative orientation of the phenyl groups, showed that when phenyl groups can attain a relative orientation close to that of the free dimer, the interaction is maximum. Among the various contributions to interaction energy, calculated using SAPT, the dispersive interaction is the major one in all the cases. The variation in the π–π interactions causes a variation about 3.5 kcal/mol in activation energies in the systems **a**-**e**. Using NCI plot, the interactions in substrate, TS and the biradical intermediate are presented. The effect of substituents of different electronic nature are assessed which shows that both types of substituents, electron-donating and electron-withdrawing, have increased the π–π interactions, however, the TS is more stabilised and hence activation energies are increased.

Acknowledgements

We acknowledge financial support from Department of Science and Technology, New Delhi in the fast track scheme to AA, and computational facility at the Department of Chemistry supported by DST special grant. SJ is grateful to UGC, Government of India, for fellowship.

References

[1] (a) L. M. Salonen, M. Ellermann, F. Diederich, *Angew. Chem., Int. Ed.*, 2011, 50, 4808.; (b) A. J. McNeil, P. Muller, J. E. Whitten, T. M. Swager, *J. Am. Chem. Soc.*, 2006, 128, 12426. (c) K. Müller-Dethlefs, P. Hobza, *Chem. Rev.* 2000, 100, 143–167.

[2] (a) S. K. Burley, G. A. Petsko, *Science*, 1985, 229, 23.; (b) S. K. Burley, G. A. Petsko, *Adv. Protein Chem*., 1988, 39, 125.; (c) S. K. Burley, G. A. Petsko, *Trends Biotechnol.*, 1989, 7, 354.
[3](a) K. O. Bornsen, H. L. Selzle, E. W. Schlag, *J. Chem. Phys*., 1986, 85, 1726.; (b) P. Hobza, H. L. Selzle, E. W. Schlag, *J. Chem. Phys*., 1990, 93, 5893.
[4](a) C. A. Hunter, *Angew. Chem., Int. Ed. Engl.,* 1993, 32*,* 1584.; (b) C. A. Hunter, *Chem. Soc. Re*v., 1994, 23, 101.; (c) F. J. Carver, C. A. Hunter, D. J. Livingstone, J. F. McCabe, E. M. Seward, *Chem. Eur. J*., 2002, 8, 2847.
[5] F. Cozzi, M. Cinquini, R. Annunziata, T. Dwyer , T. S. Siegel, *J. Am. Chem. Soc*., 1992, 114, 5729.
[6](a) S. Paliwal, S. Geib, C. S. Wilcox, *J. Am. Chem. Soc*., 1994, 116, 4497.; (b) E. Kim, S. Paliwal, C. S. Wilcox, *J. Am. Chem. Soc*., 1998, 120, 11192.
[7](a) B. H. Hong, J. Y. Lee, C. W. Lee, K. C. Kim, S. C. Bae, K. S. Kim *J. Am. Chem. Soc*., 2001, 123, 10748.; (b) B. H. Hong, S. C. Bae, C. W. Lee, S. Jeong, K. S. Kim, *Science*, 2001, 294, 348.; (c) K. S. Kim, S. B. Suh, J. C. Kim, B. H. Hong, E. C. Lee, S. Yun, P. Tarakeshwar, J. Y. Lee, Y. Kim, H. Ihm, H. G. Kim, J. W. Lee, J. K. Kim, H. M. Lee, D. Kim, C. Cui, S. J. Youn, H. Y. Chung, H. S. Choi, C. W. Lee, S. J. Cho, S. Jeong, J. H. Cho, *J. Am. Chem. Soc*., 2002, 124, 14268.; (d) P. Tarakeshwar, H. S. Choi, K. S. Kim, *Chem. Re*v., 2002, 100, 4145.
[8] (a) K. D. Schladetzky, T. S. Haque, S. H. Gellman, *J. Org. Chem*., 1995, 60, 4108.; (b) S. H. Gellman, *Chem. Rev*., 1997, 97, 1231.; (c) C. Y. Kim, P. P. Chabdra, A. Jain, D. W. Christanson, *J. Am. Chem. Soc*., 2001, 123, 9620.; (d) H. Lee, C. B. Knobler, M. F. Hawthorne, *Angew*. *Chem., Int. Ed*., 2001, 40, 3058.; (e) E. A. Meyer, R. K. Castellano, F. Diederich, *Angew*. *Chem., Int. Ed*., 2003, 42, 1210.
[9] L. S. Lerman, *J. Mol. Biol*., 1961, 3, 18.
[10] W. Saenger, *Principles of Nucleic Acid Structure*; Springer-Verlag: New York, 1984.
[11] B. H. Zimm, *J. Chem. Phys*., 1960, 33, 1349.
[12] D. M. Crothers, B. H. Zimm, *J. Mol. Biol*., 1964, 9, 1.
[13] G. Kryger, I. Silman, J. L. Sussman, *J. Physiol*., 1998, 92, 191.
[14] L. C. Gilday, S. W. Robinson, T. A. Barendt, M. J. Langton, B. R. Mullaney, P. D. Beer, *Chem. Rev*., 2015, 115, 7118.
[15] R. S. Mulliken, *J. Am. Chem. Soc*., 1952, 74, 811.
[16] C. A. Hunter, J. K. M. Sanders, *J. Am. Chem. Soc*., 1990, 112, 5525.
[17] R. A. Kumph, D. A. Dougherty, *Science*, 1993, 261, 1708,
[18] M. O. Sinnokrot, C. D. Sherrill, *J. Phys. Chem. A*, 2006, 110, 10656.
[19] S. Grimme, C. Muck-Lichtenfeld, J. Antony, *J. Phys. Chem. C,* 2007, 111, 11199.
[20] M. Rapacioli, F. Calvo, F. Spiegelman, C. Joblin, D. J. Wales, *J. Phys. Chem. A,* 2005, 109, 2487.
[21] J. Grant Hill, J. A. Platts, H.-J. Werner, *Phys. Chem. Chem. Phys.*, 2006, 8, 4072.
[22] Y. C. Park, J. S. Lee, *J. Phys. Chem. A*, 2006, 110, 5091.
[23] R. Podeszwa, R. Bukowski, K. Szalewicz, *J. Phys. Chem. A,* 2006, 110, 10345.
[24] S. Grimme, J. Antony, T. Schwabe, C. Muck-Lichtenfeld, *Org. Biomol. Chem*., 2007, 5, 741.
[25] (a)C. A. Hunter, *Angew. Chem. Int. Ed*., 1993, 32, 1584; (b) C. A. Hunter, K. R. Lawson, J. Perkins, C. J. Urch, *J. Chem. Soc. Perkin Trans.*, 2001, 2, 651.
[26] S. Tsuzuki, K. Honda, T. Uchimaru, M. Mikami, *J. Chem. Phys.*, 2006, 124, 114304.
[27] C. Gonzalez, E. C. Lim, *J. Phys. Chem. A*, 2003, 107, 10105.
[28] E. G. Hohenstein, C. D. Sherrill, *WIREs Comput. Mol. Sci*., 2012, 2, 304.
[29] E. H. Krenske, K. N. Houk, *Acc. Chem. Res*., 2013, 46, 979.
[30] (a) S. Mondal, A. Basak, S. Jana, A. Anoop, *Tetrahedron*, 2012, 68, 7202.
[31] (a) D. Ghosh, S. Jana, A. Panja, A. Anoop, A. Basak, *Tetrahedron,* 2013, 69, 8724.; (b) T. Mitra, S. Jana, P. Bhattacharya, U. K. Khamrai,, A. Anoop, A. Basak, *J. Org. Chem*., 2014, 79, 5608.
[32] M. O. Sinnokrot, W. F. Valeev, C. D. Sherrill, *J. Am. Chem. Soc*., 2002, 124, 10887.
[33] S. Grimme, *J Chem. Phys*., 2003, 118, 9095.
[34] M. O. Sinnokrot, C. D. Sherrill, *J. Phys. Chem. A*, 2004, 108, 10200.
[35] A. Hesselmann, G. Jansen, M. Schutz, *J. Chem. Phys*., 2005, 122, 14103.
[36] Y. Zhao, D. G. Truhlar *J. Phys. Chem. A*, 2005, 109, 4209.
[37] S. Tsuzuki, K. Honda, T. Uchimura, M. Mikami, K. Tanabe, *J. Am. Chem. Soc*., 2002, 124, 104.
[38] E. Kraka, D. Cremer, *WIREs Comput. Mol. Sci*., 2014, 4, 285.
[39] I. V. Alabugin, M. Manoharan, *J. Phys. Chem. A*, 2003, 107, 3363.
[40] S. Roy, A. Anoop, K. Biradha, A. Basak, *Angew. Chem., Int. Ed.*, 2011, 50, 8316.
[41] K. C. Nicolaou, G. Zuccarello, Y. Ogawa, E. J. Schweiger, T. J. Kumazawa, *J. Am. Chem. Soc*., 1998, 110, 4866.
[42] A. D. Becke, *Phys. Rev.A:At.,Mol., Opt. Phys*., 1988, 38, 3098.
[43] J. P. Perdew, *Phys. Rev. B: Condens. Matter*, 1986, 33, 8822.
[44] A. Schafer, C. Huber, R. Ahlrichs, *J. Chem. Phys*., 1994, 100, 5829.
[45] (a) A. D. Becke, E. R. Johnson, *J. Chem. Phys*., 2005, 123, 154101.; (b) E. R. Johnson, A. D. Becke, *J. Chem. Phys*., 2005, 123, 024101.; (c) E. R. Johnson, A. D. Becke, *J. Chem. Phys*., 2006, 124, 174104.
46 L. Goerigk and S. Grimme, *Phys. Chem. Chem. Phys.*, 2011, 13, 6670.
47 W. –C. Chen, N. –Y. Chang and C. -H. Yu, *J. Phys. Chem. A*, 1998, 102, 2584.
[48] A. D. Becke, *J. Chem. Phys.*, 1993, 98, 5648.
[49] P. J. Stephens, F. J. Devlin, C. F. Chabalowski, M. J. Frisch, *J. Phys. Chem.*, 1994, 98, 11623.
[50] Y. Zhao, D. G. Truhlar, *J. Chem. Phys.*, 2006, 124, 194101.
[51] S. Grimme, *J. Chem. Phys.*, 2006, 124, 34108.
[52] S. Grimme, *J. Chem.Phys.*, 2003, 118, 9095.
[53] S. F. Boys, F. Bernardi, *Mol. Phys.*, 1970, 19, 553.
[54] S. Grimme, *J. Comput. Chem*., 2004, 25, 1463.
[55] M. Parac, M. Etinski, M. Peric, S. Grimme, *J. Chem. Theor. Comput.*, 2005, 1, 1110.
[56] Orca 3.0.0, developed by Frank Neese, Max Planck Institute for Bioinorganic Chemistry, Muelheim/Ruhr, Germany.
[57] TURBOMOLE V6.5 2013, a development of University of Karlsruhe and Forschungszentrum Karlsruhe GmbH, 1989-2007, TURBOMOLE GmbH, since 2007, available from http://www.turbomole.com.
[58] G. Henkelman, B. P. Uberuaga, H. Jonsson, *J. Chem. Phys*., 2000, 113, 9901.
[59] J. Kästner, J. M. Carr, T. W. Keal, W. Thiel, A. Wander, P. Sherwood, *J. Phys. Chem. A*, 2009, 113, 11856.
[60] ChemShell 3.5, a Computational Chemistry Shell, see www.chemshell.org.
[61] J. M. Turney, A. C. Simmonett, R. M. Parrish, E. G. Hohenstein, F. A. Evangelista, J. T. Fermann, B. J. Mintz, L. A. Burns, J. J. Wilke, M. L. Abrams, N. J. Russ, M. L. Leininger, C. L. Janssen, E. T. Seidl, W. D. Allen, H. F. Schaefer, R. A. King, E. F. Valeev, C. D. Sherrill, T. D. Crawford, *WIREs Comput Mol Sci*., 2012, 2, 556.
[62] J. Contreras-Garcia, E. R. Johnson, S. Keinan, R. Chaudret, J. P. Piquemal, D. N. Beratan, W. Yang, *J. Chem. Theory Comput*., 2011, 7, 625.

[63] I. V. Alabugin, M. Manoharan, *J. Phys. Chem. A* 2003, 107, 3363.
[64] S. E. Wheeler, K. N. Houk, *J. Am. Chem. Soc.* 2008, 130, 10854.